Synthesis, Structure and Magnetic Properties of NiFe3O5

Synthesis, Structure and Magnetic Properties of $NiFe_3O_5$

Ka H. Hong,[1] Elena Solana-Madruga,[1,2] Mauro Coduri,[3] Clemens Ritter,[4] and J. Paul Attfield[1,z]

[1]Centre for Science at Extreme Conditions and School of Chemistry, University of Edinburgh, West Mains Road, Edinburgh EH9 3FD, United Kingdom
[2]Departamento de Química Inorgánica, Universidad Complutense de Madrid, Avda. Complutense sn, 28040 Madrid, Spain.
[3]European Synchrotron Radiation Facility, 71 avenue des Martyrs, Grenoble, 38000, France
[4]Institut Laue-Langevin, 38042 Grenoble, France.
[z]Corresponding Author E-mail Address [j.p.attfield@ed.ac.uk]

Abstract Text

A new $CaFe_3O_5$-type phase $NiFe_3O_5$ (orthorhombic *Cmcm* symmetry, cell parameters a = 2.89126(7), b = 9.71988(21) and c = 12.52694(27) Å) has been synthesised under pressures of 12-13 GPa at 1200 °C. $NiFe_3O_5$ has an inverse cation site distribution and reveals an interesting evolution from $M^{2+}(Fe^{3+})_2Fe^{2+}O_5$ to $Fe^{2+}(M^{2+}_{0.5}Fe^{3+}_{0.5})_2Fe^{3+}O_5$ distributions over three distinct cation sites as M^{2+} cation size decreases from Ca to Ni. Magnetic susceptibility measurements show successive transitions at 275, ~150, and ~20 K and neutron diffraction data reveal a series of at least three spin-ordered phases with evolving propagation vectors k = [0 0 0] → [0 k_y 0] → [½ ½ 0] on cooling. The rich variety of magnetically ordered phases in $NiFe_3O_5$ likely results from frustration of Goodenough-Kanamori exchange interactions between the three spin sublattices, and further interesting magnetic materials are expected to be accessible within the $CaFe_3O_5$-type family.

Introduction Text

Ferrite spinels and related materials are important for many magnetics applications and also for fundamental interest in couplings between spin, charge, orbital and lattice degrees of freedom. The parent material magnetite, Fe_3O_4, has been studied intensively due to the 125-K Verwey transition,[1] below which a complex charge and orbital ordering leads to the formation of trimerons – linear orbital molecule clusters of three Fe ions.[2] Recently further Fe_nO_{n+1} binary iron oxides and substituted derivatives have been explored following discovery that the n = 4 phase Fe_4O_5 can be recovered from high pressure high temperature (HPHT) synthesis.[3] Fe_4O_5 has an incommensurate charge order at 150 K below which dimeron and trimeron-like groups of Fe ions are formed,[4] and higher Fe_nO_{n+1} homologues with $n > 4$ have also been made at pressure.[5] Studies of n = 6 $CaFe_5O_7$ have revealed a coupled structural and magnetic transition at 360 K accompanied by charge ordering.[6,7,8]

Fe_4O_5 adopts the orthorhombic $CaFe_3O_5$ type[9] (also known as the $Sr_2Tl_2O_5$ type[10]) structure with space group *Cmcm*. This has three independent cation sites M1, M2 and M3 in a 2:1:1 ratio, where M1 and M2 form edge-sharing MO_6 octahedra channeled by triangular prisms containing the M3 site, as shown in Figure 1. MFe_3O_5 derivatives in which the M cations lie at the trigonal M3 or octahedral M1 and M2 sites may be described as having

normal or inverse cation distributions by analogy to normal and inverse spinels. Materials with large M^{2+} = Ca, Mn (and Fe) cations have normal structures and display notable electronic or magnetic properties. $CaFe_3O_5$ can be prepared at ambient pressure,[9] and lightly doped samples display long range electronic phase separation into Fe^{2+}/Fe^{3+} charge averaged and charge ordered phases with formation of trimerons in the latter.[11,12,13] The cation distributions $M3(M1)_2M2\ O_5$ over the three available sites are $Ca^{2+}(Fe^{2.67+})_2Fe^{2.67+}O_5$ in the charge averaged phase and $Ca^{2+}(Fe^{3+})_2Fe^{2+}O_5$ in the charge-ordered form. $MnFe_3O_5$, prepared under HPHT conditions, shows a rich variety of magnetic ordered states on cooling below T_C = 350 K, and Fe^{2+}/Fe^{3+} charge ordering at 60 K leads to spin reorientation.[14,15] Attempts to prepare $CoFe_3O_5$ at HPHT led to a Co-deficient product $Co_{0.6}Fe_{3.4}O_5$ in which the Co/Fe cation distribution fell between normal and inverse limits as Co^{2+} substitutes across all three cation sites.[16] $CoFe_3O_5$ shows complex magnetic behavior with weak ferromagnetism below $T_{C1} \approx 300$ K and a second transition to ferrimagnetic order at $T_{C2} \approx 100$ K. The interesting low temperature magnetic phenomena observed in these MFe_3O_5 phases reflect competition within the complex networks of Goodenough-Kanamori superexchange interactions between the various spin sublattices.[17] $MgFe_3O_5$ was also reported in a study of the Fe_4O_5 -$Mg_2Fe_2O_5$ solid solution, but the crystal structure and magnetic properties were not reported.[18] In the present work we have extended the MFe_3O_5 series to M = Ni and we report the HPHT synthesis, crystal structure studies, and magnetic properties of this new material.

Experimental

$NiFe_3O_5$ samples were prepared by HPHT reaction of NiO and Fe_3O_4 powders in a Pt capsule for 20 min in a two-stage Walker-type module. Several batches of material were synthesized at 12 or 13 GPa and 1200 °C.

HPHT reaction products were initially characterized by powder X-ray diffraction collected with a Bruker D2 diffractometer using Cu K_α radiation (15 minutes scan of $5° \leq 2\theta \leq 70°$). High resolution powder synchrotron X-ray diffraction (PSXRD) data were collected from a 8 mg $NiFe_3O_5$ sample synthesised at 12 GPa at the ID22 beamline of the ESRF with incident wavelength 0.39996 Å. A glass capillary with an outer diameter of 0.3 mm was used to contain the polycrystalline sample of approximately 8 mg. Low temperature diffraction data were collected from 90 to 471 K with an Oxford Cryosystems nitrogen cryostream. Powder neutron diffraction (PND) experiments were carried out at the D20 beamline of the ILL to study the structural and magnetic orders of $NiFe_3O_5$. Diffraction data were collected on a composite 45 mg $NiFe_3O_5$ sample from several runs at 13 GPa, using a neutron wavelength of 2.41 Å. Diffraction patterns were collected at 1.5, 110, 220, 300 and 400 K using a helium cryofurnace. The crystal and magnetic structures of $NiFe_3O_5$ were Rietveld-fitted using the FullProf Suite.[19]

A Quantum Design MPMS XL SQUID magnetometer was used to carry out magnetization measurements. The magnetic susceptibility was measured under zero field cooled (ZFC) and field cooled (FC) conditions between 2 and 400 K with an applied magnetic field of 2000 Oe. Magnetisation versus field hysteresis loops were recorded at 2 and 400 K, using an applied field between -7 and 7 T.

Results

The polycrystalline products were characterized by powder X-ray diffraction which showed that a *Cmcm* $CaFe_3O_5$-type $NiFe_3O_5$ phase was the major product, with traces of NiO and Fe_3O_4 spinel also present. The room temperature lattice parameters of $NiFe_3O_5$ are a = 2.89126(7), b = 9.71988(21) and c = 12.52694(27) Å and the cell volume is 352.04(1) $Å^3$, smaller than those of the M = Ca, Mn, Fe, and Co MFe_3O_5 phases,[11-16] consistent with the ionic size variation of M^{2+}. The crystal structure was refined against PSXRD data at temperatures between 80 and an upper limit of 450 K (as sample decomposition was observed at 471 K) giving the results shown in Figures 2-4 and supplementary material.

The $CaFe_3O_5$-type structure has three independent cation sites M1, M2 and M3 in a 2:1:1 ratio. X-ray scattering gives no elemental contrast between Fe and Ni and neutron scattering gives limited contrast as the scattering lengths are quite similar (Fe = 9.45 and Ni = 10.3 fm). Trial PND refinement of site occupancies showed only Fe at the M2 and M3 sites, and mixed Fe/Ni occupancy at the M1 site but with large refinement errors. Hence the M1 site was fixed at ($Ni^{2+}_{0.5}Fe^{3+}_{0.5}$) composition, which assumes an ideal $NiFe_3O_5$ stoichiometry. These site occupancies are corroborated by the average metal-oxygen distances at each site (Figure 4) in comparison to ideal values for Ni^{2+}–O = 2.08 Å, Fe^{2+}–O = 2.17 Å, and Fe^{3+}–O = 2.035 Å, based on Shannon high spin ionic radii.[20] The long distance at the trigonal prismatic M3 site (2.221(2) Å at 300 K) is consistent with Fe^{2+}, the short <M2-O> distance of 1.998(2) Å matches Fe^{3+}, and the intermediate <M1-O> distance of 2.077(2) Å is consistent with mixed Ni^{2+}/Fe^{3+} occupancy. $NiFe_3O_5$ thus has an inverse cation distribution on the present basis of limited PND site occupancy refinement and in particular the observed metal-oxygen distances, with Fe at the trigonal prismatic site and Ni on octahedral sites. A more detailed analysis of stoichiometry and cation distribution would require use of resonant X-ray diffraction to give high Fe/Ni scattering contrast as used for e.g. $FeNi_2BO_5$.[21]

The temperature evolution of the lattice parameters of $NiFe_3O_5$ shown in Figure 3, indicated anisotropic thermal expansion as found in the other MFe_3O_5 phases.[11,15,16] Anomalous expansion in b and contractions in a and c axes below ~275 K, relative to high temperature trends, are from magnetostrictive effects that match the onset of spin ordering as discussed below. The average M-O distances remained similar between 80 and 450 K, indicating that no $Fe^{2+/}Fe^{3+}$ charge transfer transitions take place in this temperature range.

Magnetisation measurements from a $NiFe_3O_5$ sample in Figure 5 show a divergence between ZFC and FC susceptibilities below the maximum measured temperature of 400 K. This indicates that a magnetic impurity (ferrimagnetic Fe_3O_4) is present and the similarity of the low field hysteresis features at 2 and 400 K (above and below the spin ordering temperatures for $NiFe_3O_5$ as revealed below by neutron scattering) shows that the $NiFe_3O_5$ spin ordering is not ferro- or ferri- magnetic. Discontinuities in ZFC and FC susceptibilities at $T_{N1} \approx 275$ K (consistent with the magnetostriction onset in Fig. 3), T_{N2} ~150 K, and T_{N3} ~20 K match the changes in spin ordering observed by neutron diffraction below.

Rietveld fits to the 300 and 400 K neutron diffraction patterns (Figure 6) confirm the orthorhombic *Cmcm* crystal structure. Lattice parameters and M-O distances are similar to those from the synchrotron diffraction results, but with some systematic errors due to the lower phase purity of the PND sample which contains 77(2)% $NiFe_3O_5$, 10.7(2)% Fe_3O_4 and

12.7(3)% NiO. Structural PND results are shown in supplementary material.

Comparison of the low-angle PND patterns between 1.5 and 400 K in Figure 7 reveals a complex sequence of spin transitions from the temperature evolution of $NiFe_3O_5$ magnetic reflections on cooling. Magnetic peaks appearing below the magnetisation transition at T_{N1} = 275 K can be assigned to $NiFe_3O_5$ with confidence as the magnetic impurity phases present have much higher spin ordering transitions (Fe_3O_4 has $T_C \approx 850$ K and NiO has $T_N \approx 525$ K) so their magnetic contributions do not change below 300 K. A strong (021) magnetic diffraction peak from $NiFe_3O_5$ appears between 300 and 220 K data, consistent with T_{N1} = 275 K, and this spin order has a magnetic propagation vector of k = [0 0 0]. On cooling from 220 to 110 K, the (021) intensity diminishes and a new series of incommensurate magnetic satellites appear, tentatively indexed by k = [0 k_y 0] with $k_y \approx 0.4$, showing that a second magnetic phase has emerged at T_{N2} ~150 K. At 1.5 K the (021) magnetic intensity from the k = [0 0 0] phase is no longer present but a new (½ ½ 1) peak reveals a third magnetic phase with k = [½ ½ 0] coexisting with the k = [0 k_y 0] phase. Further low temperature PND data will be needed to solve these magnetic structures and track their coexistence at low temperatures.

Discussion

The above results demonstrate that a new $CaFe_3O_5$-type phase $NiFe_3O_5$ can be synthesised under a pressure of 12-13 GPa at 1200 °C. Present samples are not phase pure showing that further optimisation of pressure-temperature conditions may be needed. As with previously discovered MFe_3O_5 analogs, $NiFe_3O_5$ adopts the orthorhombic $CaFe_3O_5$-type structure in space group *Cmcm* down to lowest temperature without any apparent structural phase transitions. However a substantial magnetostriction near 275 K is consistent with the onset of magnetic ordering, and similar effects are found in other MFe_3O_5 analogs.

The Fe/Ni site occupancies for $NiFe_3O_5$ reveal an interesting evolution between normal and inverse distributions across the MFe_3O_5 series, written as $M3(M1)_2M2O_5$ to show occupancies at the trigonal prismatic M3 and octahedral M1 and M2 sites. The normal M = Ca, Mn and Fe materials have mixed Fe^{2+}/Fe^{3+} charge states at the M1 and M2 sites but tending towards the $M^{2+}(Fe^{3+})_2Fe^{2+}O_5$ distribution as found in the charge-ordered form of $CaFe_3O_5$.[11,12] However, $NiFe_3O_5$ has site distribution $Fe^{2+}(Ni^{2+}_{0.5}Fe^{3+}_{0.5})_2Fe^{3+}O_5$ demonstrating that the normal to inverse evolution does not involve a simple exchange of M^{2+}/Fe^{2+} between M3/M2 sites, but instead proceeds by a mechanism that involves all three cation sites. Cation size appears to be the driving factor as M^{2+} moves from the trigonal prismatic M3 sites for large M to the smaller M1 octahedral site for small M, while Fe^{2+} moves from M2 to M3. This requires a concomitant shift of Fe^{3+} from M1 to M2 sites to preserve charge balance. This evolution reveals great site and charge flexibility in the $CaFe_3O_5$-type structure and other distributions are likely to be found for other $M_xFe_{3-x}O_5$ materials according the charge, size and substitution limit x for different metals M.

A variety of spin ordered states in $NiFe_3O_5$ below $T_{N1} \approx 275$ K is revealed by magnetisation measurements and powder neutron diffraction measurements at a few low temperatures (1.5, 110 and 220 K). Initial analysis based on the latter three profiles reveals at least three spin ordered phases with an evolution of propagation vector k = [0 0 0] → [0 k_y 0] → [½ ½ 0] on cooling. Further variable temperature PND data will be needed to check for

other possible intermediate magnetic phases, enable solution and refinement of the spin structures, and follow their co-existence upon cooling. It is already clear that $NiFe_3O_5$ has a comparable richness of magnetic phases to Fe_4O_5 where incommensurate spin order is also observed,[4] $CaFe_3O_5$ where different charge and spin ordered phases coexist,[11-13] and $MnFe_3O_5$ and $CoFe_3O_5$ where several k = [0 0 0] ordered phases are observed due to frustration of M and Fe spin sublattices.[14-16]

Overall it is clear that the $CaFe_3O_5$-type family of transition metal oxides offers a potentially huge variety of substituted phases based on different M^{2+}/M^{3+} transition metals and their normal or inverse site occupancy patterns, comparable to the well-known spinel or perovskite families of transition metal oxides. Each investigated MFe_3O_5 phase to date has shown interesting low temperature magnetic phenomena, usually resulting from frustration of the Goodenough-Kanamori exchange interactions between the various spin sublattices. Upper magnetic ordering transitions near 300 K also indicate possible applications as sensor or magnetocaloric materials. HPHT synthesis is likely to be required to explore these materials, although some may be accessible at ambient pressure as exemplified by the parent phase $CaFe_3O_5$.

Conclusions

In summary, the new $CaFe_3O_5$-type phase $NiFe_3O_5$ has been synthesised under a pressure of 13 GPa at 1200 °C. $NiFe_3O_5$ has an inverse cation site distribution and reveals an interesting evolution from $M^{2+}(Fe^{3+})_2Fe^{2+}O_5$ to $Fe^{2+}(M^{2+}_{0.5}Fe^{3+}_{0.5})_2Fe^{3+}O_5$ distributions over three distinct cation sites as M^{2+} cation size decreases from Ca to Ni. Magnetic susceptibility measurements reveal successive transitions at 275, ~150, and ~20 K and neutron diffraction data show a series of at least three spin-ordered phases with evolving propagation vectors k = [0 0 0] →[0 k_y 0] → [½ ½ 0] on cooling. The rich variety of magnetically ordered phases in $NiFe_3O_5$ results from frustration of Goodenough-Kanamori exchange interactions between the three spin sublattices.

Acknowledgments

We thank ERC and EPSRC for support and STFC for provision of beam time at ESRF and ILL. ILL data have doi; doi.ill.fr/10.5291/ILL-DATA.5-31-2602.

References

1. E. J. W. Verwey, *Nature*, **144**, 327 (1939).
2. M. S. Senn, J. P. Wright, and J. P. Attfield, *Nature*, **481**, 173 (2012).
3. B. Lavina, P. Dera, E. Kim, Y. Meng, R. T. Downs, P. F. Weck, S. R. Sutton, and Y. Zhao, *Proc. Nat. Acad. Sci. U.SA.*, **108**, 17281 (2011).
4. S. V. Ovsyannikov, M. Bykov, E. Bykova, D. P. Kozlenko, A. A. Tsirlin, A. E. Karkin, V. V. Shchennikov, S. E. Kichanov, H. Gou, A. M. Abakumov, R. Egoavil, J. Verbeeck, C. McCammon, V. Dyadkin, D. Chernyshov, S. van Smaalen, and L. S. Dubrovinsky, *Nat. Chem.* **8**, 501 (2016).
5 . E. Bykova, L. Dubrovinsky, N. Dubrovinskaia, M. Bykov, C. McCammon, S. V. Ovsyannikov, H. P. Liermann, I. Kupenko, A. I. Chumakov, R. Rüffer, M. Hanfland, and V.

Prakapenka, Nat. Commun. **7**, 10661 (2016).
6. C. Delacotte, F. Hüe, Y. Bréard, S. Hébert, O. Pérez, V. Caignaert, J. M. Greneche, and D. Pelloquin, *Inorg. Chem.*, **53**, 10171 (2014).
7. C. Delacotte, Y. Bréard, V. Caignaert, V. Hardy, J. M. Greneche, S. Hébert, E. Suard and D. Pelloquin, *Key Eng.Mater.,* **617**, 237 (2014).
8. C. Delacotte, Y. Bréard, V. Caignaert, V. Hardy, J. M. Greneche, S. Hébert, E. Suard and D. Pelloquin, *J. Solid State Chem.*, **247**, 13 (2017).
9. O. Evrard, B. Malaman, F. Jeannot, A. Courtois, H. Alebouyeh, and R. Gerardin, *J. Solid State Chem.* **35**, 112 (1980).
10. P. Berastegui, S. Eriksson, S. Hull, F. J. García García, and J. Eriksen, *Solid State Sci.,* **6**, 433 (2004).
11. K. H. Hong, A. M. Arevalo-Lopez, J. Cumby, C. Ritter, and J. P. Attfield, *Nat. Commun.,* **9**, 5 (2018).
12. S. J. Cassidy, F. Orlandi, P. Manuel, and S. J. Clarke, *Nat. Commun.* **10**, 5475 (2019).
13. K. H. Hong, E. Solana-Madruga, B. V. Hakala, M. Amano Patino, P. Manuel, Y. Shimakawa, and J. P. Attfield, *Phys. Rev. Mater.* **5**, 024406 (2021).
14. K. H. Hong, G. M. McNally, M. Coduri, and J. P. Attfield, *Zeitschrift für Anorg. und Allg. Chemie,* **642**, 1355 (2016).
15. K. H. Hong, A. M. Arevalo-Lopez, M. Coduri, G. M. McNally, and J. P. Attfield, *J. Mater. Chem. C,* **6**, 3271 (2018).
16. K. H. Hong, E. Solana-Madruga, M. Coduri, and J. P. Attfield, *Inorg. Chem.,* **57**, 14347 (2018).
17. J. B. Goodenough, *Magnetism and the Chemical Bond*, New York: Wiley (1963).
18. L. Uenver, A. B. Woodland, N. Miyajima, T. B. Ballaran, and D. J. Frost, *Contrib. Mineral. Petrol.* **173***,* 1 (2018).
19. J. Rodriguez-Carvajal, *Physica B,* **192,** 55 (1993).
20. R. D. Shannon, *Acta Cryst*., **A32**, 751 (1976).
21. D. A. Perkins and J. P. Attfield, *Chem. Commun.*, 229 (1991).

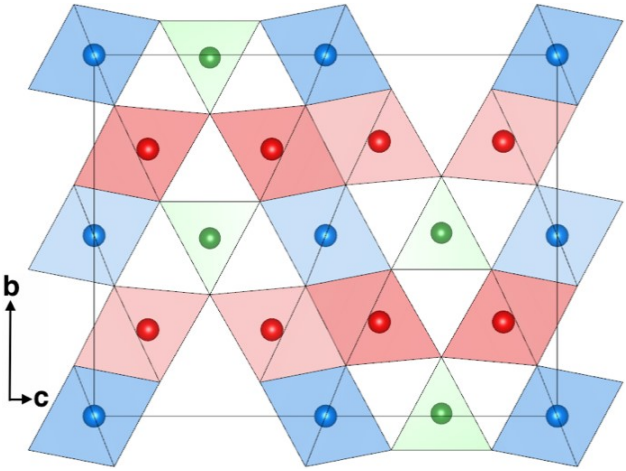

Figure 1. Polyhedral projection of the *Cmcm* structure of $NiFe_3O_5$ at 300 K with M1/M2 site octahedra shown in red/blue and M3 triangular prisms in green. Oxygen atoms (not shown) are located at the corners of polyhedra.

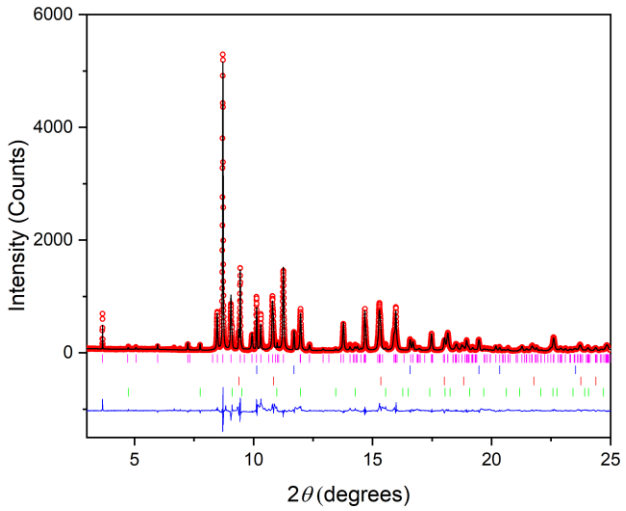

Figure 2. Rietveld fit of high resolution synchrotron x-ray diffraction pattern measured with λ = 0.399963 Å at 300 K, with pink tick marks indicating the $NiFe_3O_5$ phase [92.3(6) % by weight], blue as Pt [1.56(1)%] from the sample capsule, red as NiO [3.72(6)%] and green as Fe_3O_4 [2.48(1)%] (Residuals χ^2 = 12.9, R_{wp} = 20.9% and R_p = 17.5%). The sample was synthesised at 12 GPa and 1200 °C.

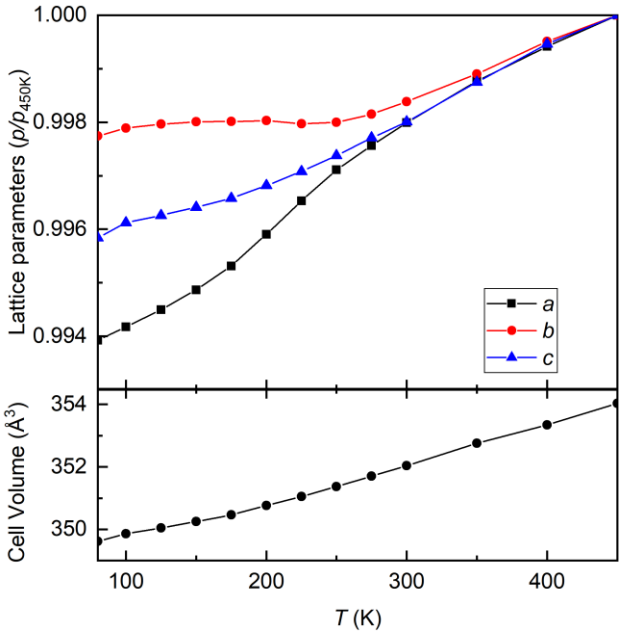

Figure 3. Changes in the lattice parameters of $NiFe_3O_5$ relative to 450 K values [a_{450} = 2.89707(7), b_{450} = 9.73561(21) and c_{450} = 12.55195(27) Å]. Cell volumes are shown below.

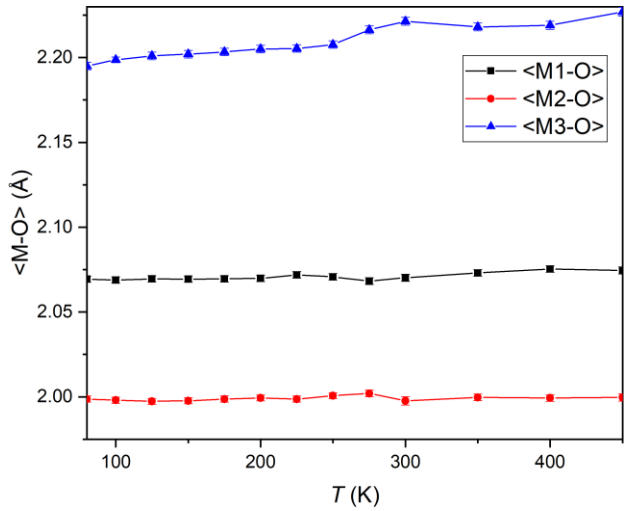

Figure 4. Changes in the average metal-oxygen distances for each of the three cation sites in the structure of $NiFe_3O_5$ from PSXRD refinements in Figure 3.

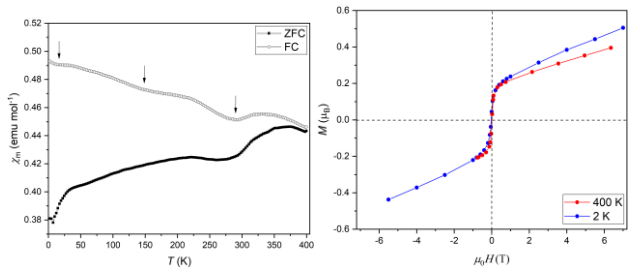

Figure 5 (Left) Zero field cooled and field cooled magnetic susceptibilities for $NiFe_3O_5$ between 2 and 400 K, with arrows indicating approximate temperatures of magnetic transitions. (Right) Magnetisation-field loops at 2 and 400 K. Data at 400 K for fields below 1 T are not shown due to spurious noise during measurement.

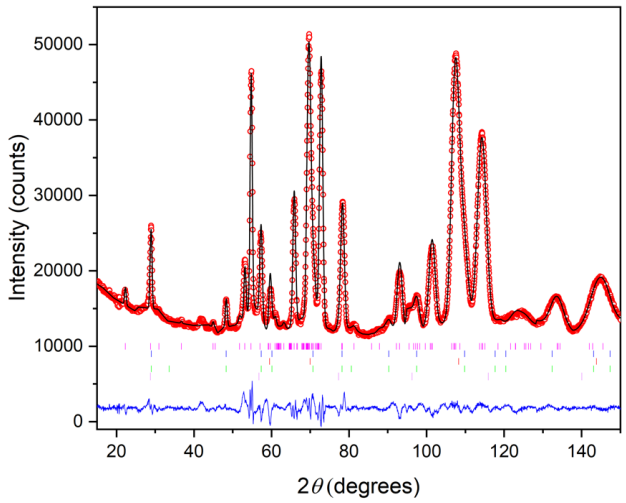

Figure 6 Rietveld fit to the 300 K neutron diffraction pattern of $NiFe_3O_5$, Tick marks from top to bottom respectively show reflections from nuclear $NiFe_3O_5$, Fe_3O_4 and NiO, and magnetic Fe_3O_4 and NiO phases (χ^2 = 11.6, R_{wp} = 7.8 % and R_p = 8.0 %).

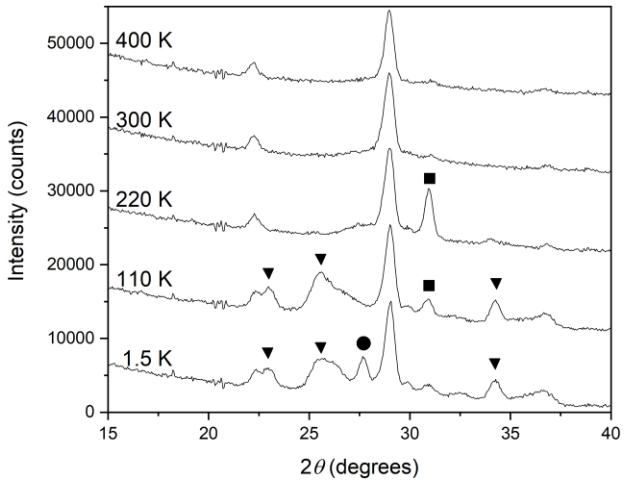

Figure 7 Temperature evolution of the low-angle neutron diffraction pattern of $NiFe_3O_5$. Magnetic peaks from spin orders with k = [0 0 0], [0 k_y 0] and [½ ½ 0] are labelled by square, triangle and circle symbols, respectively.